Low Temperature Simulation of Subliming Boundary-Layer Flow in Jupiter Atmosphere

Ching Jen Chen*
The University of Iowa, Iowa City, Iowa

A method of low temperature, approximate simulation for the sublimation of a graphite heat shield under the Jovian entry condition is studied. A set of algebraic equations was derived to approximate governing equations and boundary conditions based on the order-of-magnitude analysis. Characteristic quantities, such as wall temperature and subliming velocity, are predicted. Similarity parameters needed to simulate the most dominant phenomena of the Jovian entry flow are also given. An approximate simulation of the sublimation of a graphite heat shield is given with an air-dry ice model. The simulation with the air-dry ice model may be experimentally conducted at a lower temperature of 3000 ~ 6000 K instead of at the entry condition of 14000 K. The rate of sublimation of the graphite predicted by the present algebraic approximation agrees to the order of magnitude with extrapolated data. The limitation of the simulation method and its utility are discussed.

Nomenclature

$[DL]$ = dimensionless variables; in general, lower case letters
$[DN]$ = dimensional variables; in general, upper case letters
A = deceleration encountered by the probe
Bo_h, Bo_c = hydrogen (or air) and C_n (or CO_2) gas Boltzmann number
C_n = refers to gas evaporated from the graphite with a molecular weight of approximately 30
C_p = specific heat at constant pressure
Ev_a = evaporation parameter, the ratio of the latent heat of evaporation to the radiation flux [Eq. (25)]
E_h, E_c = Eckert number of hydrogen (or air) and C_n (or CO_2) gas [Eqs. (8) and (13)]
e_h, e_c = respectively, the ratio of hydrogen (or air) and C_n (or CO_2) gas temperature boundary layer thickness to the radius L [Eq. (23) and Fig. 1]
F_h, f_h = $[DN]$ and $[DL]$, radiation flux in hydrogen (or air) boundary layer
F_c, f_c = $[DN]$ and $[DL]$ radiation flux in C_n (or CO_2) gas boundary layer
G_h, G_c = inverse Froude number for hydrogen (or air) and C_n (or CO_2) gas [Eqs. (13) and (8)]
k = thermal conductivity
L_v = latent heat of sublimation
L = base radius of the graphite heat shield
M = molecular weight
Pr_h, Pr_c = Prandtl number for hydrogen (air) and C_n gas [Eqs. (8) and (13)]
P_e = equilibrium pressure of C_n (or CO_2) vapor [Eq. (20)]
P, p = $[DN]$ and $[DL]$ pressure defined in Eqs. (1) and (2)
Re_h = hydrogen Reynolds number [Eq. (8)]
Re_c = C_n gas Reynolds number [Eq. (13)]
R_0 = universal gas constant [Eq. (20)]
$R(X), r$ = $[DN]$ and $[DL]$, distance from the graphite surface to the axis of symmetry [Eq. (1) and Fig. 1]
T_i = temperature at hydrogen-C_n gas interface
T_∞ = temperature at the edge of hydrogen boundary layer
T_w = wall temperature or graphite surface temperature
T_m = average hydrogen (or air) temperature in the boundary layer, taken to be $(T_i + T_\infty)/2$ [Eqs. (19) and (25)]
t_h, t_c = dimensionless time [Eq. (1)]
U = X component of velocity
U_i = X component of velocity at hydrogen-C_n gas interface [Eq. (22)]
U_∞ = X component of velocity at the edge of hydrogen boundary layer
u_h, u_c = velocity components for hydrogen and C_n gas (air and CO_2) along the probe surface [Eqs. (1) and (2)]
v_h, v_c = velocity components for hydrogen and C_n gas (air and CO_2) normal to the probe surface [Eqs. (1) and (2)]
V_w = $[DN]$ velocity of sublimation [Eqs. (20) and (21)]
X, x = $[DN]$ and $[DL]$, coordinate along the surface [Eq. (1) and Fig. 1]
Y = $[DN]$, coordinate normal to the surface
y_h, y_{ht} = dimensionless Y coordinate defined in Eq. (1), used respectively for the hydrogen velocity and temperature derivatives
y_{cv} = $[DL]$, Y coordinate defined for C_n ablative layer [Eq. (2)]
y_c, y_{ct} = $[DL]$, Y coordinate defined in Eq. (2), used respectively for the C_n velocity and temperature derivatives
σ = Stefan-Boltzmann constant
δ_a = ratio of ablative layer thickness to L [Eq. (21)]
δ_h = ratio of hydrogen (or air) boundary layer thickness to L [Eq. (21)]
δ_c = ratio of C_n gas (or CO_2) boundary layer thickness to L [Eq. (21)]
ρ_∞ = density of hydrogen at the edge of the boundary layer
ρ_h, ρ_c = $[DN]$, hydrogen and C_n gas density
θ_s = $[DL]$, solid graphite temperature distribution [Eq. (3)]
θ_h, θ_c = $[DL]$, hydrogen and C_n gas temperature [Eqs. (1) and (2)]

Presented as Paper 76-473 at the AIAA 11th Thermophysics Conference, San Diego, Calif., July 14-16, 1976; submitted Sept. 23, 1977; revision received Sept. 23, 1977.

Index categories: Ablation, Pyrolysis, Thermal Decomposition and Degradation (including Refractories); Thermal Modeling and Analysis; Boundary Layers and Convective Heat Transfer—Laminar.

*Professor, College of Engineering, Energy Division. Member AIAA.

ϵ_h, ϵ_c = averaged emissivity of hydrogen (or air) and C_n gas (or CO_2)
μ = viscosity
π = ratio of the circumference of a circle to its diameter 3.14159
α = global vaporization coefficient [Eq. (20)]
τ = real time
ζ = ratio of density-viscosity product [Eq. (22)]
ϕ_h, ϕ_c = dissipation function for hydrogen (or air) and C_n (or CO_2) gas [Eqs. (7) and (12)]

Subscripts

∞ = inviscid hydrogen flow at the edge of hydrogen boundary layer
h = hydrogen gas in the entry condition and air in the simulated case
c_g = C_n gas in the entry condition, carbon dioxide gas in the simulation
c = C_n gas evaluated at a reference temperature, i.e., T_i
i = hydrogen-C_n or air-CO_2 interface
t = refers to the variable scale for temperature and radiative flux
a = sublimation layer
w = wall or graphite surface
s = condition interior to the graphite solid

I. Introduction

THIS paper examines the possibility of a low temperature simulation for a probe entering the Jovian atmosphere. In particular, the sublimation of the protective graphite heat shield and the flow and heat transfer phenomena adjacent to the heat shield are analyzed.

The probe entering the Jovian hydrogen atmosphere is preceded by a detached shock front, behind which the hydrogen shock layer may reach a temperature of 10^4 K, a speed of 10^6 cm/s, and a heating rate of 10^4 w/cm^2.[1,2] Under this condition the protective graphite heat shield sublimes as the graphite surface temperature reaches 3000 K or higher. To simulate this condition experimentally in the laboratory creates problems. First, the high temperature hydrogen wind tunnel or shock tube is difficult to build and costly. Only the recently developed Jet Propulsion Laboratory Annular Arc Accelerator shock tube[3] permits a simulation of the Jupiter entry condition, a shock velocity over 50 km/s, and 1.0 Torr of hydrogen pressure. Experimental work for outer-planetary entry today is still lacking. Secondly, the operation at such a high temperature makes measurements and observation difficult. Therefore, an approximate simulation of the sublimation of the graphite heat shield, if possible at a lower temperature with simulated material and gas, becomes a very attractive alternative.

Although several analyses and experimental works on sublimation or ablation are available, they either do not apply to the Jupiter entry condition or do not suggest details for the simulation of subliming graphite heat shield in hydrogen gas. None has suggested a low temperature simulation for Jupiter entry flow. Many sublimation and ablation experiments were performed for materials such as graphite,[9,10] camphor and dry ice,[10-12] Teflon and polyethylene,[13] and glassy material.[14] However, most of them were tested in air or nitrogen gas and did not simulate the Jupiter entry condition. Some theoretical analyses related to sublimation or ablation and simulation of Jupiter entry condition were given by Tauber and Wakefield,[2] Scala and Gilbert,[4] Kuo,[1] Lees,[5] Leibowitz and Kuo,[6] Libby,[7] and Howe and Sheaffer.[8] Scala and Gilbert[4] presented a boundary layer solution near the stagnation region for sublimation of graphite, but the analysis was done in air. Kuo,[1] adapting an approach similar to Lees[5] and Beth and Adams,[14] analyzed with a semiempirical formula the ablative heat transfer for a conical Jupiter entry probe. For simulation analysis, Howe and Sheaffer,[8] studying the flow with mass addition in the stagnation region, derived some approximate scaling parameters for an arbitrary mass addition or ablation. Similarity parameters are the Reynolds number and the ratio of the mass flux at the wall to the freestream. Libby[7] derived a set of similarity parameters required for steady ablation in air which includes Reynolds number, the ratio of molecular weight between the air and ablated material, the ratio of specific heat, the ratio of the latent heat of sublimation to the stagnation enthalpy, the ratio of a density-viscosity product, and a blowing parameter. Chen and Ostrach[15] and Kuzyk and Chen[16] presented an analysis for low temperature simulation of the melting ablation associated with Tektite and re-entry probe in hypersonic flow. Both Libby[7] and Chen and Ostrach[15] did not include the details of radiative simulation which is needed in Jupiter entry flow. In the present paper the analysis of low temperature simulation given by Chen and Ostrach[15] is extended and a method for an approximate simulation of the graphite sublimation in a Jovian hydrogen atmosphere is given.

II. Flow Region and Configuration

According to Kuo,[1] the flowfield near the probe may be considered as shown in Fig. 1 to consist of a C_n (a gas with molecular weight of 30) subliming layer on top of the graphite heat shield and a C_n boundary layer bordering the subliming layer. Above the C_n boundary layer is a hydrogen boundary layer. Between the hydrogen boundary layer and the shock front is the inviscid hydrogen flow. The inviscid hydrogen flow is considered known and given in the present study. The temperature, pressure, and velocity behind the shock front are given by Kuo[1] or can be calculated with the method outlined by Callis.[17] For example, a probe of a 120 deg blunt nose cone and a base radius of 50 cm entering the Jupiter atmosphere with a speed of 40 km/s at an angle of 6 to 15 deg produces a shock wave and behind it a temperature of 14,000 K, a pressure 2-10 atm depending on the altitude, and a hydrogen inviscid velocity of 20 km/s at the edge of the boundary layer.

The present problem is to make a simulation analysis for the flow near the graphite heat shield of the probe. We consider that the hydrogen and C_n gas in their respective layers are in equilibrium and laminar. The equilibrium assumption is adapted here so that the transport properties in each layer can be properly chosen.

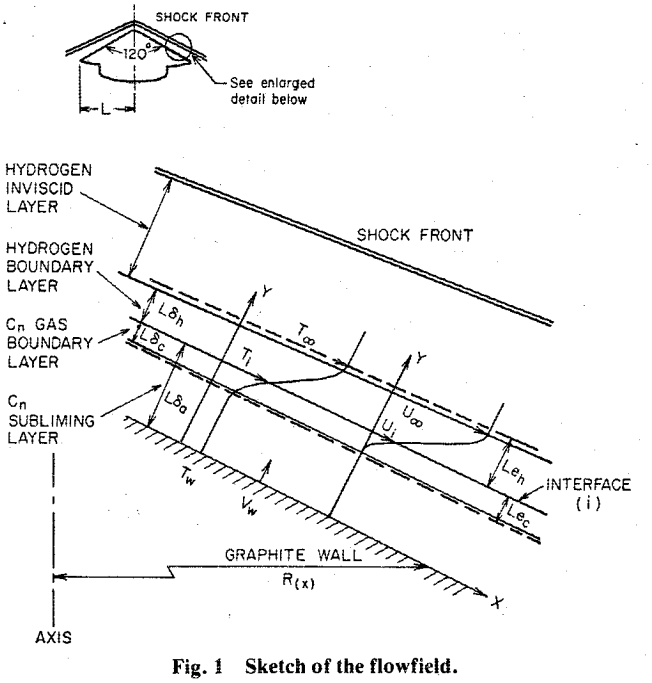

Fig. 1 Sketch of the flowfield.

III. Idea of the Algebraic Approximation

Although a complete simulation of Jupiter entry in the laboratory is not possible, it is still possible to make an approximate simulation. The basis for the approximate simulation is to simulate the most dominant phenomena or parameters of the given situation. One way to derive these dominant, similarity parameters is to perform an order-of-magnitude analysis on the governing equations and boundary conditions. The order-of-magnitude analysis may be considered as the algebraic approximation of the differential governing equations for a given problem. An example of the algebraic approximation is Prandtl's order-of-magnitude analysis for a boundary layer flow from which the ratio of the boundary layer thickness to the characteristic length of the solid boundary, δ, is found to be of the order of $1/\sqrt{Re}$. Here Reynolds number Re is the similarity or simulation parameter and $\delta = 1/\sqrt{Re}$ is the algebraic approximation of the momentum equation. In principle, this order-of-magnitude analysis or algebraic approximation may be extended to complex flows, such as the subliming boundary layer flows.

We shall systematically derive the algebraic approximation as follows. First, we choose as many characteristic quantities as needed, whether known or unknown, such that they represent the typical value for each corresponding independent and dependent variable. These characteristic variables are used to make all independent and dependent variables dimensionless. Second, whenever possible the dimensionless variables are made so that they vary from zero to one. The reason for this requirement is that when both independent and dependent variables vary from zero to one, the first derivative or gradient, with least bias, may be considered to be of the order of one. Third, all governing equations and boundary conditions are made dimensionless according to the preceding two conditions. The algebraic equations or order-of-magnitude equations are then obtained from the most dominant terms in governing equations and boundary and matching conditions. Simulation parameters are derived as a consequence of solving the unknown characteristic quantities from the equations derived by the algebraic approximation.

For the present problem (see Fig. 1) we let $L\delta_h$, Le_h, U_i, and T_i, respectively, be the unknown characteristic hydrogen velocity and temperature boundary layer thickness, and the velocity and temperature at the hydrogen-C_n gas interface. Here the subscript h denotes the hydrogen gas and ∞ the freestream condition. We let U_∞ and T_∞ be the known characteristic velocity and temperature at the edge of the hydrogen boundary layer. The following dimensionless quantities, in the lower case character, are defined for the hydrogen boundary layer:

$$u_h = U/(U_\infty - U_i) \qquad t_h = \tau(U_\infty - U_i)/L$$

$$v_h = V/\delta_h(U_\infty - U_i) \qquad r = R(x)/L, \quad x = X/L$$

$$p = P/\rho_\infty(U_\infty - U_i)^2 \qquad y_h = Y/\delta_h L$$

$$\bar{\rho}_h = \rho_h/\rho_\infty \qquad y_{ht} = Y/e_h L$$

$$\theta_h = (T_h - T_i)/(T_\infty - T_i) \qquad f_h = F_h/\epsilon_h\sigma(T_\infty^4 - T_m^4) \quad (1)$$

where y_h, y_{ht} are the Y coordinate made dimensionless, respectively, by velocity and temperature boundary layer thickness $L\delta_h$ and Le_h. The reason for this distinction is that, having done so, both velocity gradient $\partial u_h/\partial y_h$ and the temperature gradient $\partial\theta_h/\partial y_{ht}$ may be, in order of magnitude, considered to be one. All preceding dimensionless variables in Eq. (1) are now assumed to be in order of unity and vary approximately from zero to one in the hydrogen boundary layer.

Similar to these characteristic variables, we let $L\delta_c$, Le_c, and T_w be the characteristic C_n gas velocity and temperature boundary layer thickness and the wall temperature. In addition, let the subliming velocity be V_w and the total layer of the C_n gas flow $L\delta_a$. The dimensionless variables for the C_n gas boundary layer are then defined as follows

$$u_c = \frac{U}{U_i} \qquad \bar{\rho}_c = \frac{\rho_{cg}}{\rho_c} \qquad t_c = \frac{\tau U_i}{L}$$

$$v_c = \frac{V}{V_w} \qquad y_c = \frac{U}{L\delta_c} \qquad y_{cv} = \frac{V}{L\delta_a}$$

$$p = \frac{P}{\rho_\infty(U_\infty - U_i)^2} \qquad y_{ct} = \frac{Y}{Le_c}$$

$$\theta_c = \frac{(T_c - T_w)}{(T_i - T_w)} \qquad f_c = \frac{F_c}{\sigma(\epsilon_h T_m^4 - \epsilon_c T_w^4)} \quad (2)$$

The variables F_h and F_c are complex integral expressions for radiative energy flux. In order to make their dimensionless quantities f_h, f_c be of the order of one, we adapted that the typical value for F_h is the net radiative energy exchange between the hydrogen inviscid flow and hydrogen boundary layer, and F_c is that between the hydrogen boundary layer and the C_n gas layer. In defining these radiative fluxes, the temperature T_m is taken as the mean temperature of the hydrogen boundary layer or $(T_\infty + T_i)/2$. The variables y_c, y_{cv}, and y_{ct} are the normal coordinate variables used for the derivatives of velocity component u, velocity component v, and the temperature in C_n gas flow, respectively. The reason for these distinctions is again to make the derivatives $\partial u_c/\partial y_c$, $\partial v_c/\partial y_{ca}$, and $\partial\theta_c/\partial y_{ct}$ have a magnitude of one. If the interior of the probe is kept at T_s we may let the temperature and y variable in the graphite solid be

$$\theta_s = (T - T_s)/(T_w - T_s) \qquad y_s = Y/L \quad (3)$$

From Eqs. (1-3) there are nine unknown characteristic quantities, $U_i, T_i, \delta_h, e_h, \delta_c, e_c, \delta_a, V_w$, and T_w, used in defining the dimensionless variables. The knowledge of these quantites will provide a physical picture in order of magnitude for the sublimation of the graphite heat shield. These unknowns are determined from the nine approximate algebraic equations that will be derived from the governing equations and boundary conditions by the order-of-magnitude analysis in the following section.

IV. Governing Equations and Boundary Conditions

When the governing equations and necessary boundary condition are properly written, all of the information about the flow and heat transfer of the problem are contained in them. If we can correctly apply the algebraic approximation to them, we will be able to extract the most dominant relation from them. From these algebraic equations the characteristic quantities and similarity parameters needed for simulation are then obtained.

The governing equations and boundary conditions, in the dimensionless variables just defined, are written as follows. For the hydrogen boundary layer:

Continuity equation

$$\frac{\partial\bar{\rho}_h}{\partial t_h} + \frac{\partial}{\partial x}(r\bar{\rho}_h u_h) + \frac{\partial}{\partial y_h}(r\bar{\rho}_h v_h) = 0 \quad (4)$$

Momentum equations

$$\bar{\rho}_h\left(\frac{\partial u_h}{\partial t_h} + u_h\frac{\partial u_h}{\partial x} + v_h\frac{\partial u_h}{\partial y_h}\right) = \frac{\partial p_h}{\partial x} + G_h\left[1 - \left(\frac{dr}{dx}\right)^2\right]^{1/2}$$

$$+ \frac{1}{Re_h\delta_h^2}\left(\frac{\partial^2 u_h}{\partial y_h^2} + \delta_h^2\frac{\partial^2 u_h}{\partial x^2} + \ldots\right) \quad (5)$$

$$\bar{\rho}_h\left(\frac{\partial v_h}{\partial t_h}+u_h\frac{\partial v_h}{\partial x}+v_h\frac{\partial v_h}{\partial y_h}\right)=-\frac{1}{\delta_h^2}\frac{\partial p_h}{\partial y_h}+\frac{\mathrm{d}r}{\mathrm{d}x}\frac{G_h}{\delta_h}$$

$$+\frac{1}{Re_h\delta_h^2}\left(\frac{\partial^2 v_h}{\partial y_h^2}+\delta_h^2\frac{\partial^2 v_h}{\partial x^2}+\ldots\right) \tag{6}$$

Energy equation

$$\bar{\rho}_h\left(\frac{\partial\theta_h}{\partial t_h}+u_h\frac{\partial\theta_h}{\partial x}+\frac{\delta_h}{e_h}v_h\frac{\partial\theta_h}{\partial y_{ht}}\right)$$

$$=\frac{1}{Re_hPr_he_h^2}\left(\frac{\partial^2\theta_h}{\partial y_{ht}^2}+e_h^2\frac{\partial^2\theta_h}{\partial x^2}\right)+\frac{E_h}{Re_h\delta_h^2}\Phi_h$$

$$-\frac{1}{Bo_he_h}\left(\frac{\partial f_h}{\partial y_{ht}}+e_h\frac{\partial f_h}{\partial x}\right)+E_h\frac{Dp_h}{Dt_h} \tag{7}$$

where

$$\Phi_h=2\left(\frac{\partial u_h}{\partial x}\right)^2+2\left(\frac{\partial v_h}{\partial y_h}\right)^2+\left(\frac{1}{\delta_h}\frac{\partial u_h}{\partial y_h}+\delta_h\frac{\partial v_h}{\partial x}\right)^2$$

Here the coordinate system is considered fixed with respect to the graphite heat shield. Thus, any deceleration, A, encountered by the probe is represented by $G_h=AL\rho_\infty/(U_\infty-U_i)^2$, the inverse Froude number in the momentum equation. X and Y, respectively, are the coordinates along and normal to the surface of the graphite heat shield. The dots (...) in Eqs. (5) and (6) denote other viscous terms of no greater magnitude than the two terms in the brackets. Re_h, Pr_h, and Bo_h are similarity parameters defined as follows.

$$Re_h=\frac{(U_\infty-U_i)L\rho_\infty}{\mu_\infty} \qquad \text{hydrogen Reynolds number}$$

$$Pr_h=\frac{C_{p\infty}\mu_\infty}{K_\infty} \qquad \text{hydrogen Prandtl number}$$

$$E_h=\frac{(U_\infty-U_i)^2}{C_{p\infty}(T_\infty-T_i)} \qquad \text{hydrogen Eckert number}$$

$$Bo_h=\frac{C_{p\infty}\mu_\infty(U_\infty-U_i)(T_\infty-T_i)}{\epsilon_h\sigma(T_\infty^4-T_m^4)} \qquad \text{hydrogen Boltzmann number} \tag{8}$$

For the C_n gas boundary layer:

Continuity equation

$$\frac{\partial\bar{\rho}_c}{\partial t_c}+\frac{\partial}{\partial x}(r\bar{\rho}_cu_c)+\left[\frac{V_w}{U_i\delta_a}\right]\frac{\partial}{\partial y_{cv}}(r\bar{\rho}_cv_c)=0 \tag{9}$$

Momentum equations

$$\bar{\rho}_c\left(\frac{\partial u_c}{\partial t_c}+u_c\frac{\partial u_c}{\partial x}+\left[\frac{V_a}{U_i\delta_c}\right]v_c\frac{\partial u_c}{\partial y_c}\right)=\left[\frac{\rho_\infty(U_\infty-U_i)^2}{\rho_cU_i^2}\right]$$

$$\times\left[-\frac{\partial p_c}{\partial x}+G_c\left(1-\left(\frac{\mathrm{d}r}{\mathrm{d}x}\right)^2\right)^{1/2}\right]+\frac{1}{Re_c\delta_c^2}\left(\frac{\partial^2 u_c}{\partial y_c^2}\right.$$

$$\left.+\delta_c^2\frac{\partial^2 u_c}{\partial x^2}+\ldots\right) \tag{10}$$

$$\bar{\rho}_c\left(\frac{\partial v_c}{\partial t_c}+u_c\frac{\partial v_c}{\partial x}+\left[\frac{V_w}{U_i\delta_a}\right]v_c\frac{\partial v_c}{\partial y_{cv}}\right)$$

$$=\left[\frac{\rho_\infty(U_\infty-U_i)^2}{\rho_cU_iV_a\delta_a}\right]\left(-\frac{\partial p_c}{\partial y_{cv}}+G_c\delta_a\frac{\mathrm{d}r}{\mathrm{d}x}\right)$$

$$+\frac{1}{Re_c\delta_a^2}\left(\frac{\partial^2 v_c}{\partial y_{cv}^2}+\delta_a^2\frac{\partial^2 u_c}{\partial x^2}+\ldots\right) \tag{11}$$

Energy equation

$$\bar{\rho}_c\left(\frac{\partial\theta_c}{\partial t_c}+u_c\frac{\partial\theta_c}{\partial x}+\left[\frac{V_w}{U_ie_c}\right]v_c\frac{\partial\theta_c}{\partial y_{ct}}\right)$$

$$=\frac{1}{Re_cPr_ce_c^2}\left(\frac{\partial^2\theta_c}{\partial y_{ct}^2}+e_c^2\frac{\partial^2\theta_c}{\partial x^2}\right)+\frac{E_c}{Re_c^2\delta_c^2}\Phi_c$$

$$-\frac{1}{Bo_ce_c}\left(\frac{\partial f_{cy}}{\partial y_c}+\frac{\partial f_{cx}}{\partial x}e_c\right)+E_c\frac{Dp_c}{Dt_c} \tag{12}$$

where

$$\Phi_c=2\left(\frac{\partial u_c}{\partial x}\right)^2+2\left[\frac{V_w}{U_i\delta_a}\right]\left(\frac{\partial v_c}{\partial y_{cv}}\right)^2+\left[\frac{V_w}{U_i}\right]\left(\frac{\partial v_c}{\partial x}+\frac{1}{\delta_c}\frac{\partial u_c}{\partial y_c}\right)^2$$

Here, as in the case of the hydrogen layer, the parameters G_c, Re_c, Pr_c, E_c, and Bo_c are defined as follows

$$G_c=AL\rho_c/U_i^2 \qquad \text{inverse } C_n \text{ Froude number}$$

$$Re_c=U_iL\rho_c/\mu_c \qquad C_n \text{ Reynolds number}$$

$$Pr_c=C_{pc}\mu_c/k_c \qquad C_n \text{ Prandtl number}$$

$$E_c=\frac{U_i^2}{C_{pc}(T_i-T_w)} \qquad C_n \text{ Eckert number}$$

$$Bo_c=\frac{C_{pc}\mu_cU_i(T_i-T_w)}{\epsilon_h\sigma(T_m^4-T_w^4)} \qquad C_n \text{ Boltzmann number} \tag{13}$$

The boundary conditions are written in terms of the dimensionless variables. The boundary conditions at the outer edge (denoted by the subscript ∞) of the hydrogen boundary layer are all of unit order or

$$\theta_h=\theta_\infty=0(1) \qquad u_h=u_\infty=0(1) \tag{14}$$

In addition to the symmetric condition at the stagnation point, both the hydrogen gas and the C_n gas layers must be matched at their interface. With the subscript i denoting the condition at the interface, we have

Continuity

$$u_{hi}=[U_i/(U_\infty-U_i)]u_{ci}$$

$$v_{hi}=[(U_i\delta_c)/(U_\infty-U_i)\delta_h]v_{ci} \tag{15}$$

Tangential stress

$$\left(\frac{\partial u_h}{\partial y_h}+\delta_h^2\frac{\partial v_h}{\partial x}\right)_i=\left[\frac{\mu_c\delta_hU_i}{\mu_\infty\delta_c(U_\infty-U_i)}\right]\left(\frac{\partial u_c}{\partial y_c}+\delta_c^2\frac{\partial v_c}{\partial x}\right)_i \tag{16}$$

Normal stress

$$p_h+\frac{2}{Re_h}\left(\frac{\partial v_h}{\partial y_h}\right)_i=p_c+\frac{2}{Re_c}\left[\frac{\rho_cU_i^2}{\rho_\infty(U_\infty-U_i)^2}\right]\left(\frac{\partial v_c}{\partial y_t}\right)_i \tag{17}$$

Energy transfer

$$\left(\frac{\partial\theta_c}{\partial y_{ct}}\right)_i=\left[\frac{k_he_c(T_\infty-T_i)}{k_ce_h(T_i-T_w)}\right]\left(\frac{\partial\theta_h}{\partial y_{ht}}\right)_i \tag{18}$$

At the graphite wall, in addition to the no-slip condition $u_c=0$, the balance of radiative, conductive, and evaporative

energy transfer in dimensionless form is

$$\left[\frac{\epsilon_h\sigma(T_m^4-T_w^4)}{\rho_c V_w L_v}\right]f_c-\left[\frac{k_c(T_i-T_w)}{Le_e\rho_c V_w L_v}\right]\frac{\partial\theta_c}{\partial y_{ci}}$$

$$=-\left[\frac{k_s(T_w-T_\infty)}{L\rho_c V_w L_v}\right]\frac{\partial\theta_s}{\partial y_s}+\bar{\rho}_c v_{cw} \tag{19}$$

with

$$T_m=(T_i+T_\infty)/2$$

Where the first term of the equation represents the radiative heat transfer, the second and the third are, respectively, the conduction term on the vapor and solid side. The last term represents the heat of evaporation of the graphite heat shield. The mass rate of evaporation, $\bar{\rho}_c v_{cw}$, is related to the actual pressure on the wall P, the wall temperature T_w, and other physical constants of the material and is given by Kuo[1] as

$$\bar{\rho}_a v_{cw}=\frac{\alpha(P_e-P)}{\rho_c V_w}\sqrt{\frac{M}{2\pi R_0 T_w}} \tag{20}$$

where

$$\log_{10}p_e=11.494-\frac{43630}{T_w(in\ K)}$$

α is the global vaporization coefficient and is taken to be 0.145, as suggested by Kuo,[1] which is approximately the average values given by Zavitsanos[18] and Bishop and DiCristina.[19] P_e, in atmosphere, is the graphite equilibrium pressure at T_w, while P is the surface partial pressure, taken to be the pressure acting outside the boundary layer and assumed known. M/R_0 is the molecular weight divided by the universal gas constant.

V. Equations and Solutions of Algebraic Approximation

There are nine unknown characteristic quantities to be determined; namely, two velocity boundary layer thicknesses δ_h and δ_c, two temperature boundary layer thicknesses e_h and e_c, the sublimating velocity V_w, the subliming layer thickness δ_a, the interface velocity and temperature U_i and T_i, and the wall temperature T_w. They will be determined from nine algebraic equations derived from the differential governing equations. In the algebraic approximation we will retain the most dominant term in each governing equation and boundary condition. In the order of magnitude approximation, we set all the variables and their first derivatives equal to one. This leaves a set of algebraic equations relating the characteristic quantities in square brackets. The resulting approximate equations will contain some of the preceding unknown and other similarity parameters previously defined.

The algebraic equations are just a crude approximation of both the original governing equations and boundary conditions. Nevertheless they retain the essential physics of the phenomenon.

To derive the algebraic equations we first examine Eq. (9). Here in order for the flow to remain two dimensional, $[V_w/U_i\delta_a]$ must be of the order of one since all the derivatives in Eq. (9) are made to be of the order of one. Furthermore, since the convective term in Eqs. (5) and (10) is of order one, the magnitude of the highest derivative term in Eqs. (5) and (10), i.e., the viscous term, must be at least of equal order of one if the boundary conditions (14) and (15) are to be satisfied. Therefore, if we consider that the second derivative terms are of order one we must require algebraic relations from Eqs. (5) and (10), equating convective and viscous terms, as

$$1/Re_h\delta_h^2=1 \qquad 1/Re_c r_c^2=1$$

The continuity Eq. (9) also gives

$$V_w/U_i\delta_a=1$$

Here the value of one on the right-hand side means an order of magnitude of one. These relations lead to, similar to the Prandtl's boundary layer relations,

$$\delta_h=[(U_\infty-U_i)L\rho_\infty/\mu_\infty]^{-1/2}$$

$$\delta_c=(U_iL\rho_c/\mu_c)^{-1/2}$$

$$\delta_a=V_w/U_i \tag{21}$$

The boundary conditions for the momentum Eqs. (5, 6, 10, and 11), are given in Eqs. (14-16). From these boundary conditions, if we require that the tangential stress must be continuous at the interface, we then need $[\mu_c\delta_h U_i/\mu_\infty\delta_c(U_\infty-U_i)]$ in Eq. (16) to be of order one or combining with Eq. (21)

$$U_i/U_\infty=(1+\zeta)^{-1} \qquad \zeta=(\rho_c\mu_c/\rho_\infty\mu_\infty)^{1/2} \tag{22}$$

This is the algebraic approximation of the matching conditions (16) and (17). Equation (22) shows that the interfacial velocity U_i is a function of the freestream velocity U_∞ and the ratio of $\rho\mu$ product ζ between the hydrogen and C_n gas. It should be mentioned that ζ ratio is a well-known ratio in the literature of two-phase flow problems such as film condensation[20] or film boiling.[21] Indeed it is also a similarity parameter suggested by Libby.[7]

Turning to energy Eqs. (7) and (12), we reason that if one is to satisfy the thermal boundary conditions, Eqs. (14, 18 and 19), the highest derivative term or the conduction term in Eqs. (7) and (12) must be kept in the approximation. By equating the conduction term to the convection term, one obtains the following relations

$$e_h=(Re_hPr_h)^{-1/2} \qquad e_c=(Re_cPr_c)^{-1/2} \tag{23}$$

These two relations are also well known in determining the temperature boundary layer thickness. When either the dissipation or radiation term becomes greater than the convection term, i.e., large Eckert number or small Boltzmann number, there will exist a dissipation or radiation layer within the temperature boundary layer. To find this layer is to equate the conduction term respectively to the dissipation or radiation term. This will be examined later.

The thermal boundary conditions are given by Eqs. (14, 18, and 19). In order that the energy transfer be continuous at the hydrogen-C_n gas interface, we require that the ratio $[k_he_c(T_\infty-T_i)/k_ce_h(T_i-T_w)]$ in Eq. (18) be of order one, or an algebraic equation of

$$T_i/T_\infty=[1+(T_w/T_\infty)(k_he_c/k_ce_h)]/[1+(k_he_c/k_ce_h)] \tag{24}$$

This equation determines the temperature at the hydrogen-C_n gas interface. The interface temperatutr, T_i, now depends on both the freestream and wall temperature, as well as the ratio of the thermal conductivity k_h/k_c and the ratio of the two temperature boundary layer thicknesses e_c/e_h. Since the ratio e_c/e_h depends on Reynolds numbers Re_h and Re_c and on Prandtl numbers Pr_h and Pr_c, the interface temperature, T_i, is a complex function of the flow and thermal boundary conditions and many fluid properties. In Eq. (24), if the wall temperature is maintained at a fixed and controlled temperature (for example, by a cooling process inside the graphite heat shield), then the interface temperature is determined from the equation. Otherwise, when the surface temperature T_w is an unknown quantity, it must be determined from the boundary condition at the wall, Eq. (19). In Eq. (19) we assume that the radiative flux dominates the heat conduction

because of the high freestream temperature in the present problem. Therefore, the radiative flux is largely absorbed by the latent heat of sublimation. Thus, under the algebraic approximation we have

$$[\epsilon_h \sigma (T_m^4 - T_w^4)/\rho_c V_w L_v] = 1$$

or

$$\frac{V_w}{U_\infty} = \frac{1}{Ev_a}\left(\frac{T_m^4 - T_w^4}{T_\infty^4}\right) \tag{25}$$

where

$$Ev_a = \rho_c L_v U_\infty / \epsilon_h \sigma T_\infty^4$$

Since Eq. (25) introduces an additional unknown of the evaporating velocity V_w, one needs one more equation for V_w before T_i and T_w can be solved from Eqs. (24) and (25). To this end we have Eq. (20), which describes the thermodynamic relation between the sublimating velocity V_w, the graphite temperature T_w, the partial pressure at the surface P, and the equilibrium or saturated vapor pressure P_e. W may rewrite Eq. (20) as

$$T_w = \alpha^2 (P_e - P)^2 (M/2\pi R_0 \rho_c^2 V_w^2) \tag{26}$$

where the equilibrium vapor pressure, P_e, at T_w, is given by the other equation in Eq. (20). One may see that if T_w is fixed, then T_i is given by Eq. (24) and V_w is determined by Eq. (25). Equation (26) then determines what the wall pressure P must be. However for the Jupiter entry problem, P is determined when a trajectory of the probe is selected. In this case T_w cannot be predetermined or fixed. Thus, T_i, T_w, and the evaporating velocity V_w are determined from coupled Eqs. (24-26) and can be solved by trial and error iteration. In the case of simulation, Eq. (20) will have to be replaced by the thermodynamic relation of the material or gas under consideration. In other words, the equation relating the equilibrium pressure to the wall temperature will take on different constants as given in Ref. 22. Since Eq. (26) merely describes the thermodynamic relation of a particular substance, it serves only to specify the state, say, T_w, V_w, or P, in which the sublimation will take place. Therefore, Eq. (26) needs in low-temeprature simulation to be replaced by the equation describing the relation among T_w, V_w, and P for the simulated substance.

VI, Simulation Parameters and Characteristic Values

Equations (21-26) are equations that determine the nine unknown characteristic quantities, $\delta_c, \delta_h, \delta_a, e_c, e_h, T_i, T_w, U_i$, and V_w. Aside from the thermodynamic variables in Eq. (26), the following dimensionless parameters determine the previous unknown variables. These dimensionless parameters can be grouped into two categories.

$$\text{Dynamic parameters: } Re_h,\ Re_c,\ \zeta$$

$$\text{Thermal parameters: } Pr_h,\ Pr_c,\ k_h/k_c,\ Ev_a \tag{27}$$

These are the most essential similarity parameters needed for an approximate simulation of the sublimating boundary layer flow in the Jovian atmosphere. These parameters and the characteristic quantities can be calculated once the conditions of hydrogen inviscid flow, $U_\infty, T_\infty, \rho_\infty, P$, and the characteristic length of the probe, L, are given. The other similarity parameters, such as Eckert, Froude, and Boltzmann numbers, are of secondary importance under the algebraic approximation.

We calculate now the case for a Jupiter entry probe having a cone angle of 120 deg with a base radius of 50 cm. The conditions behind the shock front (Fig. 1) in the hydrogen inviscid flow is

$U_\infty = 2\times 10^6$ cm/s $\quad P_\infty = 8$ atm

$T_\infty = 1.4\times 10^4$ K $\quad \rho_\infty = 1.4\times 10^{-6}$ g/cm^3

$\mu_\infty = 10^{-3}$ g/s cm $\quad k_\infty = 1.7\times 10^{-2}$ cal/s cm K

$Pr_h = 0.8$ $\quad \epsilon_h = 0.8$

For the C_n gas flow at 8 atm and 5000 K, we have

$\rho_c = 6\times 10^{-4}$ g/cm^3 $\quad \mu_c = 10^{-3}$ g/s cm K

$k_c = 6\times 10^{-4}$ cal/s cm K $\quad Pr_c = 0.7$

$L_v = 6.5\times 10^3$ cal/g $\quad \epsilon_c = 0.8$

$\alpha = 0.145$ $\quad M = 30$

Here the value for the latent heat of vaporization L_v and the coefficient of evaporation for Eq. (26) are suggested by Kuo.[1] The other values are taken as the most representative ones from reports of Kuo,[1] Scala,[14] Yos,[23] and Aroeste and Benton.[24] From these data the characteristic quantities and similarity parameters are calculated and listed in Table 1. In calculating these values the viscosity-density ratio ζ was first evaluated. From this the interface velocity U_i/U_∞ and hence Reynolds number for both hydrogen and C_n velocity boundary layer, Re_h and Re_c, were calculated from Eqs. (8, 13, and 22). T_i, T_w, V_w are obtained from Eqs. (24-26) by trial-and-error calculation. In the process, Prandtl numbers Pr_h and Pr_c, the ratio of thermal conductivity k_∞/k_c, and evaporation parameter Ev_a, were also tabulated. Then T_w, which leads to the prediction of both V_w and T_i from Eqs. (24) and (25), is varied until Eq. (26) is satisfied. The sublimating layer thickness then follows from Eq. (21).

From the calculated characteristic values we may construct an approximate physical picture for the sublimation of a graphite heat shield in the Jupiter entry. This is given in Fig. 2 where boundary layer thickness, velocity, and temperature are given to the scale, as predicted by the algebraic approximation. From Fig. 2 or Table 1, we see that δ_a of the subliming C_n gas layer is larger than both the hydrogen and C_n gas boundary layer δ_h and δ_c. The temperature boundary layer e_h and e_c is slightly greater than the respective velocity boundary layer δ_h and δ_c, because the Prandtl numbers for both hydrogen and C_n gas are less than one. T_i (5581 K) is

Table 1 Similarity parameters and characteristic quantities

Similarity parameters	Jupiter probe, hydrogen-graphite	Simulated model, air-dry ice
ζ	6.153	1.38
Re_c	8.36×10^6	8.3×10^6
Re_h	1.2×10^6	0.93×10^5
Pr_c	0.7	0.79
Re_h	0.8	0.73
k_∞/k_c	28.3	16.3
Ev_a	187.3	187.3
Characteristic quantities		
U_i/U_∞	0.14	0.42
δ_c	3.45×10^{-4}	3.45×10^{-4}
δ_h	9×10^{-4}	3.28×10^{-3}
δ_a	8.53×10^{-3}	3.28×10^{-3}
e_c	4.13×10^{-4}	3.88×10^{-4}
e_h	1×10^{-3}	3.8×10^{-3}
V_a/U_∞	1.2×10^{-3}	1.36×10^{-3}
T_i/T_∞	0.399	0.711
T_w/T_∞	0.346	0.07

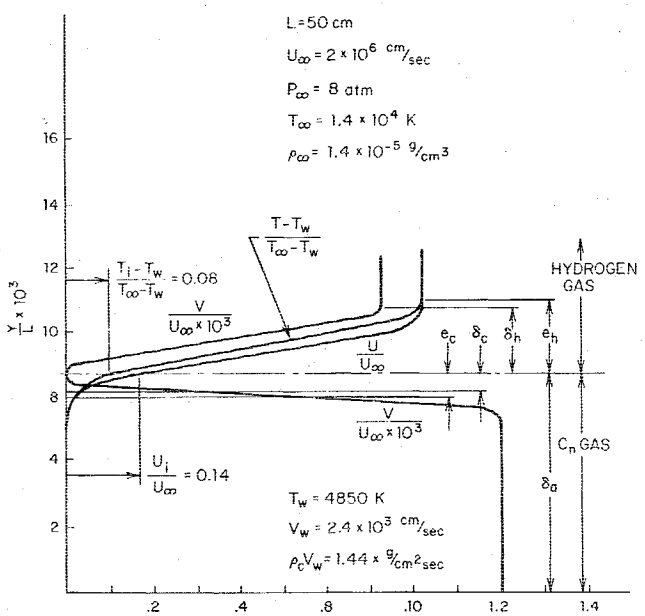

Fig. 2 Order-of-magnitude analysis for sublimation of graphite heat shield.

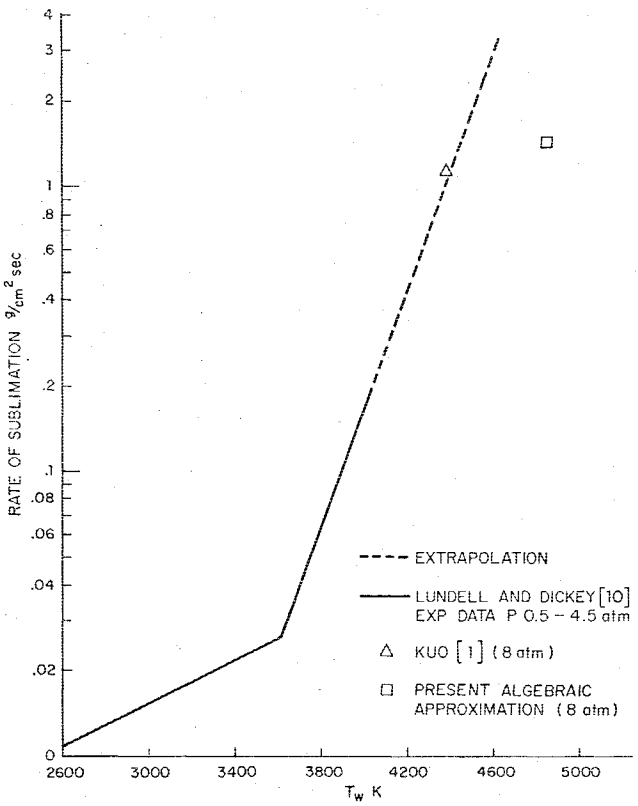

Fig. 3 Comparision of the predicted rate of sublimation and experimental data.

predicted to be close to T_w (4840 K) showing a good blockage effect by the subliming C_n layer. The interface velocity U_i reaches 2.8×10^5 cm/s or 14% of the freestream hydrogen velocity. This implies that C_n gas moves rather slowly compared with hydrogen gas. The reason for the relatively low U component velocity in the C_n gas layer is because the molecular weight, $M = 30$, of the C_n gas is much larger than that of the hydrogen gas, $M_h = 2$. Because of the large density difference, C_n gas gives a large inertial resistance to hydrogen gas flow. In making a trial-and-error calculation for T_w and, V_w, one will find that V_w is very sensitive to T_w and, therefore, to the equilibrium vapor pressure P_e. The wall temperature had to be determined to within ± 50 deg K if all three of Eqs. (24-26) are to be satisfied. From the present calculation we predict a wall temperature of 4850 K, an evaporating velocity of 2.4×10^3 cm/s, and a rate of sublimation $\rho_c V_w = 1.44$ g/cm^2 s. This compares favorably with Kuo's[1] calculation which gives $T_w = 4400$ K and 1.15 g/cm^2 s. In a recent test of graphite sublimation by Lundell and Dickey,[10] they reported experimental results for the pressure varying between 0.5 to 4.5 atm and wall temperature ranging from 2600 to 4000 K. If we extrapolate their data (Fig. 3), Kuo's[1] calculation is in execellent agreement with the experimental data, while the present calculation based on the algebraic approximation predicts a slightly higher wall temperature but with a good rate of sublimation. The intent of the present study is to investigate the possibility of a low temperature simulation. The preceding comparison confirms the validity of the algebraic approximation.

We examine now other similarity parameters neglected in the algebraic approximation, namely, Froude, Eckert, and Boltzmann numbers. For example, the inverse Froude number for the hydrogen boundary layer is negligibly small with an order of 10^{-11} even though the Jupiter probe may encounter 100 ~ 300 g of deceleration. Therefore, instability of flow due to deceleration or Taylor instability will be of secondary importance. On the other hand, Eckert number for both hydrogen and C_n gas are large in the Jupiter entry flow. This implies that dissipative heating may be important in the flow and may be the major factor in modifying the temperature distribution in both boundary layers. The value of Boltzmann number calculated is of an order 10^8 which makes the radiative term in the energy Eqs. (7) and (12), of secondary importance. This means that while radiation is important in supplied energy for the sublimation of the graphite heat shield, it is relatively ineffective to modify the temperature distribution in both boundary layers.

VIII. Low Temperature Simulation

The present method of simulation is valid in the region between the shock wave to the graphite heat shield. We now consider the possibility of a low temperature simulation using different materials and gases. For an approximate simulation of the Jupiter entry, the similarity parameters given in Eq. (27) are most important. If these parameters are approximately simulated, then the phenomenon of the sublimation of the graphite heat shield is simulated whether the simulation uses the hydrogen gas and graphite or other gases and materials for sublimation. We outline the procedure of calculation for the simulation first and then illustrate with an example.

1) One must examine several possible combinations of sublimation material and gases to simulate the graphite heat shield and hydrogen gas. For example, they may be dry ice-air, dry ice-helium, dry ice-steam, or camphor-nitrogen combination.

2) Once the combination is chosen, the four similarity parameters, ζ, the ratio of viscosity-density product and k_h/k_c the ratio of thermal conductivity, and two Prandtl numbers Pr_h, Pr_c, are calculated for a chosen temperature, pressure, and density behind the shock wave, such that they approximately match the corresponding values given in Table 1. The condition in front of the shock wave may be calculated from the condition required behind the shock wave if a supersonic tunnel or a shock tube is chosen to do the simulation. The simulation of the subsonic region near the stagnation point may alternatively be simulated in a subsonic tunnel without simulating a shock front.

3) The similarity parameter Ev_a given in Eq. (25), which simulates the balance of the radiative energy flux to the rate of energy absorbed by the sublimation, must now be simulated. We observe that Ev_a defined in Eq. (25) includes the density ρ_c, latent heat L_v, emissivity ϵ_h, and freestream temperature

and velocity T_∞ and U_∞. As the freestream temperature T_∞ and simulation material are already chosen in the first step of the procedure, one may proceed to vary the freestream velocity U_∞, such that the Ev_a value is simulated.

4) With U_∞ now determined, the interface velocity U_i can be obtained from Eq. (22).

5) Knowing $U_>$ and U_i we can now simulate the two Reynolds numbers Re_h and Re_c by choosing the size of the simulated model L. If this size turns out to be unsuitable for the simulation facility available, the procedure is repeated from the second step by varying the simulation temperature and pressure range.

6) The other characteristic quantities, such as T_w, V_w, T_i, and sublimation layer thickness δ_a are calculated as before by trial-and-error procedure from the algebraic equations [Eqs. (21-25)] while the thermodynamic relation, Eq. (26), is now replaced by the similar equation for the simulated sublimation material.

As an example, the air-dry ice combination is chosen for the simulation under the Jupiter entry condition as given in Table 1. If the experiment is conducted in one atmosphere and at a substantially lower temperature of 3000 K, then a 66.4 cm radius dry-ice model is needed in a wind tunnel with 1.31 m/s of air velocity. For this condition the dry ice will sublime at 210 K at a rate of 0.045 g/cm^2 s.

In Table 1 we see that thermal similarity parameters Pr_h, Pr_c, k_h/k_c and Ev_a are closely simulated, while the dynamic similarity parameters ζ, Re_h, and Re_c are only approximately simulated. C_n gas Reynolds number Re_c is simulated exactly, but hydrogen gas Reynolds number Re_h and ζ are undersimulated. This is a result of the difference in the density (or molecular weight) between air and carbon dioxide being much smaller than that between the hydrogen and C_n gas. The difference shows in the ratio of the viscosity-density product ζ which, in turn, affects the interface velocity. The ratio U_i/U_∞ for Jupiter entry is 0.14 while the air-dry ice simulation gives 0.42. For this consideration the helium-dry ice combination is better than the air-dry ice combination since helium gas will have a smaller molecular weight resembling that of the hydrogen gas. In freestream temperature and pressure conditions similar to those just considered, the helium-dry ice model will give a value of 2.5 for ζ.

Probably the most difficult part of the simulation, particularly the low temperature simulation, is the radiative flux. In the simulation the radiative effect is included in the similarity parameter, Ev_a, where the radiative heat flux is lumped into $\epsilon_h \sigma T_\infty^4$. Air at low temperature is a nonradiatively participating medium. Therefore, to simulate the radiative energy flux to the sublimating material, some artificial radiation must be devised. This may be accomplished in two ways. First, if the simulation is conducted at a high temperature, then some radiatively participating gas, such as CO_2 or H_2O, may be mixed with air to achieve the necessary radiative flux. In this respect a steam-dry ice combination may be considered. If the simulation is conducted in a shock tube which normally has a small test section but allows for high temperature operation, one may simulate Ev_a at a high temperature. The high temperature simulation will, in turn, lead to a higher simulated gas velocity than that given by a low temperature simulation. Secondly, if the simulation is conducted at a low temperature the radiative heat flux to the sublimating material must be supplied by an external radiation source, such as a laser heater or radiation lamp. The radiative heating can be independently controlled for its power output such that the Ev_a is simulated. If the radiative heating is Q, then the freestream temperature T_∞ can be taken to be $[Q/\epsilon_h \sigma]^{1/4}$ and used in Eqs. (24) and (25). This method is particularly attractive, since the low temperature simulation can be held at a gas temperature where the radiation is negligible. Furthermore, at different levels of radiative heating the similarity of Ev_a may still be simulated by choosing a suitable freestream velocity U_∞. The added flexibility for selecting U_∞ allows us to determine a suitable model size in the simulation, as long as we satisfy the similarity of Reynolds number. The larger the radiative flux is used the greater the simulated velocity as required from the similarity of Ev_a and hence the smaller the model size as required to simulate Re_h and Re_c can be made.

VIII. Conclusions

The analysis presented permits one to approximately simulate in a lower temperature environment the high temperature subliming boundary layer on the heat shield entering the Jupiter atmosphere. The flexibility of the low temperature simulation and the low cost in conducting the experiment makes the method attractive in investigating many problems associated with Jupiter entry. Investigations of heat shield recession rate, surface features, transition in the subliming boundary layer, stability of the hydrogen-C_n gas interface, flow separation, and particulate mass loss are some examples.

Acknowledgment

The author would like to thank Floyd Livingston of the Aerophysics Section, Jet Propulsion Laboratory, for his suggestion to examine the low temperature simulation technique and Ta Jim Kuo for providing the needed data. This work was supported in part by Jet Propulsion Laboratory Contract Agreement No. 560015.

References

[1] Kuo, T. J., "Ablative Heat Transfer of a Conical Jupiter Entry Probe," Jet Propulsion Lab. Interim Rept., Aerophysics Sec., Oct. 1971.

[2] Tauber, M. E. and Wakefield, R. M., "Heating Environment and Protection during Jupiter Entry," *Journal of Spacecraft and Rocket*, Vol. 8, June 1971, pp. 630-636.

[3] Leibowitz, L. P., "Attachment of Jupiter Entry Shock Velocity," *AIAA Journal*, Vol. 13, March 1975, pp. 403-404.

[4] Scala, S. M. and Gilbert, L. M., "Sublimation of Graphite at Hypersonic Speeds," *AIAA Journal*, Vol. 3, Sept. 1965, pp. 1635-1644.

[5] Lees, L., "Similarity Parameters for Surface Melting of a Blunt Nosed Body in High Velocity Gas Stream," *ARS Journal*, Vol. 29, May 1959, pp. 345-354.

[6] Leibowitz, L. P. and Kuo, T. J., "Ionization Nonequilibrium Heating During Outer Planetary Entries," *AIAA Journal*, Vol. 14, Sept. 1976, pp. 1324-1329.

[7] Libby, P. A., "Similarity Parameters for Subliming Bodies in Hypersonic Flow," General Applied Science Labs, Inc., Westbury, N.Y., TR-453, Sept. 1964.

[8] Howe, J. T. and Sheaffer, Y. S., "Mass Addition in the Separation Region for Velocity up to 50,000 Feet per Second," NASA Tech. Note TR R-207, Aug. 1964.

[9] Metzger, J. W., Engel, M. J., and Diaconis, N. S., "Oxidation and Sublimation of Graphite in Simulation Re-Entry Environments," *AIAA Journal*, Vol. 5, March 1967, pp. 451-459.

[10] Lundell, J. H. and Dickey, R. R., "Ablation of Graphitic Materials in the Sublimation Regime," *AIAA Journal*, Vol. 13, Aug. 1975, pp. 1073-1085.

[11] Stock, H. W., "Surface Patterns on Subliming and Liquefying Ablation Materials," *AIAA Journal*, Vol. 13, Sept. 1975, pp. 1217-1223.

[12] Lipfert, F. and Genovese, J., "An Experimental Study of the Boundary Layers on Low-Temperature Subliming Ablators," *AIAA Journal*, Vol. 9, July 1971, pp. 1330-1337.

[13] Vajvodich, N. S., "The Performance of Ablative Materials in a High-Energy Partially Dissociated Frozen Nitrogen Stream," NASA Tech. Note D-1205, 1962.

[14] Bethe, H. A. and Adams, M. C., "A Theory for the Ablation of Glassy Materials," *Journal of Aerospace Sciences*, Vol. 26, June 1959, pp. 321-326.

[15] Chen, C. J. and Ostrach, S., "Low Temperature Simulation of Hypersonic Melting Ablation and the Observed Waves," *AIAA Journal*, Vol. 9, June 1971, pp. 1120-1125.

[16] Kuzyk, W. and Chen, C. J., "Investigation of Simulated Melting Instability Waves Near Stagnation Region in Hypersonic Flow," *AIAA Journal*, Vol. 10, Nov. 1972, pp. 1505-1509.

[17] Callis, L. B., "Coupled Nongray Radiating Flows about Long Blunt Bodies," *AIAA Journal*, Vol. 9, April 1971, pp. 553-559.

[18] Zavitsanos, P. D., "The Vaporization of Pyroltic Graphite," *Dynamic Mass Spectrometry*, edited by D. Price and J. E. Williams, Vol. 1, 1970.

[19] Bishop, W. M. and DiCristina, V., "The Combustion and Sublimation of Carbon at Elevated Temperature," AIAA Paper 68-759, Los Angeles, Calif., June 1968.

[20] Rutunaprakarn, O. and Chen, C. J., "Effect of Lighter Non-condensable Gas on Laminar Film Condensation Over a Vertical Plate," *International Journal of Heat and Mass Transfer*, Vol. 18, 1975, pp. 993-996.

[21] Nishikawa, K. and Ito, T., "Two-Phase Boundary-Layer Treatment of Free Convection Film Boiling," *International Journal of Heat and Mass Transfer*, Vol. 9, 1966, pp. 103-115.

[22] "Handbook of Chemistry and Physics," *The Chemical Rubber Co.*, 52nd ed. Chapt. D, P. D-151, 1971.

[23] Yos, J. M., "Transport Properties of Nitrogen, Hydrogen, Oxygen, and Air to 30,000 K," TM-63-7, Research and Advanced Development Div., AVCO, Wilmington, Mass., March 1963.

[24] Aroeste, H. and Benton, W., "Emissivity of Hydrogen Atoms at High Temperature," *Journal of Applied Physics*, Vol. 7, Feb. 1956, pp. 117-121.